Submarine groundwater discharge as a source of nutrients and trace metals in a Mediterranean Bay (Palma Beach, Balearic Islands)

Valentí Rodellas[1*], Jordi Garcia-Orellana[1,2], Antonio Tovar-Sánchez[3], Gotzon Basterretxea[3], José M. López-Garcia[4], David Sánchez-Quiles[3], Ester Garcia-Solsona[1], Pere Masqué[1,2].

[1] Institut de Ciència i Tecnologia Ambientals, Universitat Autònoma de Barcelona, 08193 Bellaterra, Spain

[2] Departament de Física, Universitat Autònoma de Barcelona, 08193 Bellaterra, Spain

[3] IMEDEA (CSIC-UIB), Miquel Marques 21, 07190 Esporles, Spain

[4] Instituto Geológico y Minero de España (IGME), Ciudad Querétaro, 07007 Palma de Mallorca, Spain.

*Corresponing author: valenti.rodellas@uab.cat (+34 93 581 1191)

ABSTRACT

Submarine Groundwater Discharge (SGD) from a detrital coastal aquifer into the adjacent marine environment was investigated in a Mediterranean bay (Palma Beach, Balearic Islands). In this region, agriculture and tourism are potential sources of groundwater contamination. A survey in the Palma Beach revealed N, Fe and chlorophyll *a* enhancement associated to areas of preferential groundwater discharge from the nearby coastal aquifer. Groundwater sampling from wells and coastal piezometers indicated high concentrations of dissolved inorganic nitrogen and Fe (up to 2800 μmol L^{-1} and 8200 nmol L^{-1}, respectively). Other nutrients, such as DIP, and trace elements were not particularly elevated, which is attributed to the adsorptive characteristics of the carbonated composition of this detrital aquifer and/or the lack of major sources. Cross-shore gradients of ^{223,224,226}Ra isotopes indicated a diffusive shore-based source of these radionuclides and allowed estimates of a SGD flow of 56000 ± 13000 m^3 d^{-1}. Our results show that SGD is a major pathway for delivering DIN (1900 mmol m^{-1} d^{-1}), dissolved Fe (4.1 mmol m^{-1} d^{-1}) and, to a lesser extent, DIP (16 mmol m^{-1} d^{-1}) into the nearshore waters. This allochtonous input may sustain a substantial phytoplankton biomass resulting in an onshore-offshore gradient (4.7 – 7.1 mg m^{-3} in nearshore seawater as compared with <1 mg m^{-3} in offshore stations). This work emphasizes the relevance of SGD-driven nutrient and trace metal inputs in the regulation of nearshore phytoplankton communities of oligotrophic areas.

Key words: Submarine Groundwater Discharge (SGD), Nitrogen, Phosphorus, iron, metals, Mediterranean, Radium isotopes

1. INTRODUCTION

Submarine groundwater discharge (SGD) includes any flow of water on continental margins from the seabed to the coastal ocean, regardless of fluid composition or driving force (Burnett et al., 2003). Thus, SGD encompasses fresh groundwater and former seawater circulating through the coastal aquifer or the "subterranean estuary" (Moore, 1999). Many coastal ecosystems are suspected to rely to some extent on nutrients and essential micronutrients (e.g. Fe, Co, Zn) supplied by SGD. In particular, SGD has been recognized as an important source of nutrients (e.g. Garcia-Solsona et al., 2010a), dissolved inorganic carbon (Cai et al., 2003) or trace metals (e.g. Beck et al., 2007a) to coastal waters. Major nutrients, and particularly nitrate, are the most studied constituents of SGD in different locations (e.g. Santos et al., 2008; Weinstein et al., 2011) and are considered the principal drivers of ecological changes in coastal communities (Howarth et al., 2000). Supply of these nutrients in the form of dissolved inorganic nitrogen (DIN) or dissolved inorganic phosphorus (DIP) into coastal areas may favor phytoplankton growth, drive short-term changes in the coastal microalgal community composition and result in deleterious effects such as coastal eutrophication or harmful algae blooms (e.g. Garcés et al., 2011; Lee et al., 2010; Valiela et al., 1990). Less is known about the fluxes of other limiting elements, such as trace metals and particularly Fe, through groundwater discharge. A few studies have documented trace metal fluxes into the ocean associated to SGD (e.g. Beck et al., 2007a; Jeong et al., 2012; Windom et al., 2006), and studies reporting SGD-driven fluxes of trace metals into the Mediterranean Sea are nonexistent.

The relevance of SGD as a driver of coastal ecosystem changes may be particularly significant in oligotrophic and semi-arid regions, such as the Mediterranean Sea. In these systems, other external nutrient sources are scarce and surface runoff may be

70 insignificant for large time periods (i.e. dry season), making SGD a major and stable
71 pathway for freshwater and terrestrial compounds to enter into the coastal ocean
72 (Shellenbarger et al., 2006; UNESCO, 2004). The inputs of nutrients and essential
73 micronutrients supplied by SGD may represent the major source of nutrients sustaining
74 nearshore plankton communities.

75 Despite the evident importance of SGD in the regulation of coastal biogeochemical
76 cycles, there is a lack of detailed assessments of the relevance of SGD as a source of
77 nutrients and trace metals into oligotrophic seas. This is partially attributed to the fact
78 that SGD is a coastal process that is often patchy, diffuse and temporally variable with
79 multiple driving forces (Burnett et al., 2003). This inherent complexity makes
80 geochemical tracers more suitable than direct methods for the evaluation of SGD fluxes.
81 In this context, Ra isotopes (^{223}Ra, ^{224}Ra, ^{226}Ra and ^{228}Ra) have been successfully
82 applied as tracers to quantify SGD fluxes (and also turbulent mixing and water
83 residence times), since they are enriched in groundwater relative to coastal seawater and
84 behave conservatively once released in the marine environment (e.g. Beck et al., 2007b;
85 Moore et al., 2006; Rodellas et al., 2012).

86 In the present study, we determine the magnitude of SGD into Palma Beach
87 (Majorca, Balearic Islands) using Ra isotopes, and associated fluxes of nutrients and
88 trace metals with the aim of evaluating the contribution of SGD to nearshore nutrient
89 pools and establishing potential linkages between SGD and coastal productivity. This
90 study represents a comprehensive study of SGD in a detrital Mediterranean site and it is
91 the first work where the magnitude of trace metal inputs through SGD into the
92 Mediterranean Sea is evaluated.
93

2. METHODS

2.1. Study area: Palma Beach

Palma Beach is a carbonated sediment beach extending ~5km in the south-east of the Palma Bay, located in the southwestern part of the island of Majorca (Balearic Islands, NW Mediterranean; Fig. 1a). The Palma Bay is the primary touristic resort in the Balearic Islands and one of the main touristic destinations in the Mediterranean Sea. The population in the area is concentrated along the coastal zone (~ 450 x 10^3 permanent inhabitants), seasonally peaking in summer. The city of Palma, located in the NW area of the bay, accommodates most of this population and also supports the main commercial harbor in the island (Fig. 1b).

Climate conditions in the area are typically Mediterranean with mild winter temperatures (mean ~9.3 ºC) and dry and warm summers (24.6 ºC). Average annual rainfall in the area is 410 mm and surface fresh water flow to Palma Bay is restricted to sporadic events following heavy rains. The inland system (Palma Basin) corresponds to a sedimentary basin filled with marine and continental deposits, from the Miocene to the Quaternary, extending over an area of ~ 370 km^2 (Candela et al., 2008; Nielsen et al., 2004). There are two main aquifers in the basin: (i) a deep Miocene carbonate aquifer formed by limestones, extending along the north boundary of the basin and not present in the Palma Beach area, and (ii) a shallow unconfined detrital aquifer, from the PlioQuaternary, occupying most of the sedimentary basin (Fig. 1b). This shallow aquifer, which is impacted by human activities (i.e. agriculture, industry or urban activities), mainly discharges through a dune-beach system (now urbanized) located in the Palma Beach, at the southeastern region of the Palma Basin. This sandy area hides a paleo-valley that represents a preferential groundwater flowpath to the sea (N. Courtois, F. Brissaud, D. Crespí, P. Lachassagne, P. Le Strat and P. Xu, unpubl). The shallow

119 unconfined detrital aquifer could thus represent a major SGD source to the study site.
120 Coastal circulation is mainly regulated by wind forcing which can result in poor
121 renewal during summer (e.g. Jordi et al., 2011). The tides have a minor influence on
122 coastal waters, as the tidal range is less than 0.3 m. The bathymetry varies smoothly (~
123 1% slope) reaching 15 m water depth at about 2000 m offshore, with the isobaths nearly
124 parallel to the shoreline (Fig. 1b). Environmental monitoring surveys reveal that Palma
125 Beach presents signs of eutrophication related to the availability of nutrients and
126 microalgal accumulation in nearshore waters (PHIB, 2008).
127
128 **2.2. Sample collection**
129 A detailed survey focused on nearshore waters of Palma Beach was carried out
130 from 17th to 21st of May 2010 to determine the magnitude of SGD, its associated flux of
131 nutrients and trace metals, and the potential connections between SGD and the
132 enhanced coastal phytoplankton biomass. Three detailed transects running
133 perpendicular to the shoreline (T1 to T3) were sampled (Fig. 1c). Each transect
134 consisted of 8 stations at approximately 5, 125, 250, 500, 750, 1000, 1250 and 2000 m
135 from the shoreline. An additional station located farther offshore (~4000 m from the
136 shoreline) was sampled in transect T2 as a reference of open seawater conditions.
137 Surface water samples for Ra, nutrients, trace metals (only in 9 stations) and Chl*a* were
138 collected at each station. Salinity and temperature at different depths were measured in
139 situ using a YSI 556 multiparameter probe. Samples for Ra analysis were stored in 60L
140 containers. Nutrients and trace metals were sampled at 1 m water depth using a
141 peristaltic pump. Seawater was pumped through acid-cleaned Teflon tubing coupled to
142 a C-flex tubing (for the Cole-Parmer peristaltic pump head), filtered through an acid-
143 cleaned polypropylene cartridge filter (0.22 μm; MSI, Calyx®), and collected in a 13

144 mL PE tubes for nutrients and 0.5 L low-density polyethylene plastic bottle for metals
145 (Tovar-Sánchez, 2012). Water samples of 240 mL for Chl*a* analysis were filtered
146 through Whatman GF/F glass fiber filters. Nutrients and Chl*a* samples were kept frozen
147 until their analysis.

148 Groundwater was sampled from four coastal wells and five piezometers distributed
149 along the beach shoreline. Each piezometer station was sampled at different depths and
150 slightly different locations. A submersible pump was used to collect samples from wells
151 for Ra isotopes. For trace metals and nutrients a 5 L Niskin bottle was used. A Retract-
152 A-Tip piezometer system (AMS, Inc.) connected to a peristaltic pump was used to
153 sample Ra isotopes in porewater. Porewater samples for trace metal and nutrient
154 analysis were collected at several depths using a multi-pore piezometer made of non-
155 metal components (Beck et al., 2007a). Notice that the term "groundwater" is used in
156 this paper for both fresh-water from wells and porewater from piezometers, as it is
157 commonly considered in SGD research. Three sediment samples were collected
158 throughout the Palma Bay to characterize the concentration of long-lived Ra isotopes
159 (^{226}Ra and ^{228}Ra) in bay sediments.

160 In addition to the sampling focused on Palma Beach, in June 2009 a sampling
161 survey covering a grid of 37 stations throughout Palma Bay was conducted to
162 characterize the distribution of trace metals in the study site. Trace metals in this
163 previous sampling were collected as described above.

164

165 **2.3. Analytical methods**

166 Ra isotopes were measured by filtering large volume seawater samples (10 L for
167 piezometers and 60 L for coastal seawater and well samples) through MnO_2-
168 impregnated acrylic fiber (hereafter, Mn-fiber) at a flow rate <1 L min^{-1} to

169 quantitatively extract Ra isotopes (Moore and Reid, 1973). In the laboratory, the Mn-
170 fibers were rinsed with Ra-free deionized water, partially dried (Sun and Torgersen,
171 1998) and placed in a Radium Delayed Coincidence Counter (RaDeCC) to quantify the
172 short-lived Ra isotopes (^{223}Ra and ^{224}Ra; Moore and Arnold, 1996). Uncertainties in
173 activities of ^{223}Ra and ^{224}Ra were estimated following Garcia-Solsona et al. (2008).
174 Then, the Mn-fibers were ashed (820ºC, 16 h), ground and transferred to counting vials
175 to determine the long-lived Ra isotopes by gamma spectrometry using a well-type high-
176 purity Ge detector. Gamma measurements were carried out after aging the samples for a
177 minimum of 3 weeks. ^{226}Ra and ^{228}Ra were determined using the ^{214}Pb and ^{228}Ac
178 photopeaks at 352 and 911 keV respectively. All Ra activities were decay corrected to
179 the date of collection. To quantify ^{226}Ra and ^{228}Ra in sediments, samples were dried,
180 crushed and hermetically sealed in calibrated geometries, to be analyzed using a coaxial
181 Ge gamma spectrometer as described above.
182 Concentrations of dissolved NO_3^- and NO_2^- (DIN) and PO_4^{3-} (DIP) were determined
183 with an autoanalyzer (Alliance Futura) using colorimetric techniques (Grasshoff et al.,
184 1983). The accuracy of the analysis was established using Coastal Seawater Reference
185 Material for Nutrients (MOOS-1, NRC-CNRC; recoveries obtained were 107 ± 11 %,
186 107 ± 6 % and 100 ± 6 % for PO_4^{3-}, $NO_3^-$and NO_2^-, respectively). Trace-metal samples
187 were acidified to pH<2 with ultrapure grade HCl (Merck) in a class-100 HEPA laminar
188 flow hood and stored for at least 1 month before extraction. Dissolved (<0.22 μm)
189 metals (Fe, Ni, Cu, Zn, Mo, Pb) were preconcentrated by the APDC/DDDC organic
190 extraction method and analyzed by ICP-MS (PerkinElmer ELAN DRC-e) (Tovar-
191 Sánchez, 2012). The accuracy of the analysis was established using Coastal Seawater
192 Reference Material for trace metals (CASS-4 and NASS-5, NRC-CNRC; recoveries
193 obtained ranging from 96.1 % to 112.1 %, for Zn and Fe, respectively). The

194 concentration of Chl*a* in water samples was determined through fluorometric analysis
195 (Parsons et al., 1984). The filters were extracted in 90% acetone overnight and
196 fluorescence was measured on a Turner Designs fluorometer calibrated with pure Chl*a*
197 (Sigma Co.).
198

199 **3. RESULTS**

200 **3.1. Palma Beach nearshore water characterization**

201 Seawater salinities were relatively homogeneous (37.5 ± 0.2) throughout the three
202 transects but a very narrow band with lower salinity was observed in the first tens of
203 meters from the shoreline. Salinities at this band were lower at T1 (34.4) and to a lesser
204 extent, at T3 (36.3). Salinity variations in depth (greater than 0.1) were detected at five
205 stations near the shoreline, with fresher salinities at the surface layer than those
206 measured in deeper waters (down to 3 - 4 m depth).

207 Nearshore waters showed significant enrichments of ^{223}Ra, ^{224}Ra and ^{226}Ra relative
208 to samples offshore (Krustal-Wallis test was applied to compare nearshore (<250 m)
209 and offshore (>2000 m) samples: $p \sim 0.01$) (Fig. 2). Ra concentrations decreased with
210 distance offshore (Fig. 2), suggesting that most Ra inputs occurred at the shoreline. The
211 three transects surveyed presented comparable patterns and Ra activities suggesting
212 homogeneous Ra inputs along the shoreline and/or rapid homogenization driven by
213 currents flowing parallel to the shore. Onshore-offshore gradients of ^{228}Ra were not
214 evident (Kruskal-Wallis, $p = 0.19$), as nearshore activities ranged from 4.2 to 8.5 dpm
215 $100L^{-1}$, which is in the range of ^{228}Ra activities measured offshore (3.2 – 5.7 dpm $100L^{-1}$).
216 The fairly constant ^{228}Ra distribution suggests a lack of major inputs of this isotope
217 at the shoreline, most likely due to the low concentrations in ^{228}Ra measured in
218 inflowing SGD (see section 3.4.), thus preventing the use of this radionuclide as a SGD
219 tracer at this setting. Although the tidal cycle could affect the Ra distribution observed
220 (Knee et al., 2011), we considered that the low tidal range of Palma Bay (< 0.3 m) had a
221 minor influence on the Ra concentrations measured in seawater.

222 Significant differences in DIN concentrations were observed between nearshore and
223 offshore waters (Krustal-Wallis test, $p < 0.01$), suggesting a terrestrial input of DIN

224 (Fig. 3). Some of the shoreline concentrations were very high (> 64 μmol L^{-1}) and
225 corresponded to samples with low salinities and high Ra activities. DIP concentrations
226 were higher than 0.05 μmol L^{-1} in only a few samples, all of them located nearshore and
227 mainly along T2 (Fig.3).
228 Concentrations of Fe (3.0 – 6.0 nmol L^{-1}), Ni (2.9– 5.6 nmol L^{-1}), Cu (5.9 - 13 nmol
229 L^{-1}), Zn (3.3 – 10 nmol L^{-1}), Mo (81 - 160 nmol L^{-1}) and Pb (0.28 – 0.40 nmol L^{-1}) were
230 relatively constant in nearshore waters of Palma Beach. No particular spatial
231 distribution of trace metals could be delineated with the limited set of samples we
232 collected (n=9). However, the sampling conducted in 2009 allowed us to assess the
233 general distribution of trace metals in the entire Palma Bay (Fig 4). Concentrations of
234 Mo and Ni were homogeneous and showed little contrast between nearshore and
235 offshore waters. Concentrations of Cu, Pb and Zn were remarkably higher in the NW
236 region of the bay, near the harbor and the city of Palma, whereas Fe was enriched at
237 nearshore waters of Palma Beach, at the SE of the bay.
238 The spatial distribution of phytoplankton biomass along the three transects revealed
239 significant onshore enhancements of Chl*a* (4.7 – 7.1 mg m^{-3}) relative to offshore
240 concentrations (1.1 - 1.5 mg m^{-3} farther than 2000 m offshore) (Krustal-Wallis test, $p \sim$
241 0.01) (Fig. 3). These biomass concentrations are high when compared with summer
242 coastal waters of the Majorca island (0.1-0.7 mg m^{-3}) and in the range of the beaches
243 experiencing eutrophication in this region (Basterretxea et al., 2007; 2010).
244
245 **3.2. Groundwater characterization**
246 Groundwater sampled from wells revealed some exchange between the aquifer and
247 the sea, with salinity values ranging from 2.1 to 3.8. Salinities of porewater samples
248 obtained with coastal piezometers varied widely, showing a notable gradient between

249 the NW (6.2-19.6) and the SE (24.1 – 31.0) boundaries of the beach. The lower
250 salinities measured at the NW region are consistent with the existence of a Paleocene
251 valley that funnels the outflow from the shallow aquifer in this area (Fig. 1b).
252 Activities of Ra isotopes measured in groundwater either from piezometers or wells
253 ranged from 2.7 to 23 dpm $100L^{-1}$ for ^{223}Ra, 23 to 110 dpm $100L^{-1}$ for ^{224}Ra, 3.5 to 61
254 dpm $100L^{-1}$ for ^{226}Ra, 4.5 to 100 dpm $100L^{-1}$ for ^{228}Ra, most of them exceeding the
255 activities measured in nearshore seawater (Fig. 5). Similar activities of Ra isotopes in
256 SGD have been reported in other studies conducted in Western Mediterranean islands
257 (e.g. Garcia-Solsona et al., 2009; Moore, 2006). The high salinity porewaters collected
258 from the SE area of the Palma Beach showed the highest activities of ^{223}Ra, ^{224}Ra and
259 ^{228}Ra, whereas the highest activities of ^{226}Ra were measured in fresher porewaters from
260 the NW region, where the shallow aquifer connects with the sea (Fig. 5). Porewater
261 samples collected from all the shoreline piezometers showed a fairly constant
262 $^{224}Ra/^{223}Ra$ activity ratio (5.5 ± 0.3; $r^2 = 0.833$; $p < 0.001$; Fig. 5a), suggesting that the
263 transit time of porewaters through coastal sandy sediments was long enough to allow
264 the water to be enriched with the Ra desorbed from the sediments. No linear correlation
265 was found between ^{228}Ra and ^{226}Ra (Fig. 5b). Indeed, minimal influence of the sediment
266 is expected for long-lived Ra, as the Ra signals acquired from a previous solid matrix
267 (i.e. an aquifer) do not significantly decay and the concentration of long-lived Ra
268 isotopes in the sediments may be low due to their low production rates from their parent
269 isotopes (Hancock and Murray, 1996).
270 Nitrate concentrations in the aquifer were very high (200 - 1600 μmol L^{-1} in wells
271 and 0.05 - 2800 μmol L^{-1} in beach piezometers), with higher concentrations generally
272 measured in fresher waters (Fig. 6). Unlike nitrate, phosphate concentrations were very
273 low in fresh groundwater (either from wells or fresh piezometers) and the highest

phosphate concentrations (up to 5.2 μmol L^{-1}) were measured in mid-salinity porewater samples from piezometers (Fig. 6).

Concentrations of Fe (20 – 8145 nmol L^{-1}), Ni (5.7 – 15 nmol L^{-1}), Cu (0.6 - 110 nmol L^{-1}), Zn (7.0 – 1600 nmol L^{-1}) and Pb (0.1 – 6.5 nmol L^{-1}) in coastal porewaters and wells markedly exceeded those measured in seawater (Fig. 6). Porewaters were particularly enriched in Fe, with concentrations 1 to 3 orders of magnitude higher than in seawater, suggesting that SGD may be an important source of this metal to the coastal sea, as previously reported for other regions (e.g. Windom et al., 2006; Jeong et al., 2012). In contrast, concentrations of Mo (4.3 - 320 nmol L^{-1}) in porewaters and wells were comparable to those measured in coastal seawater.

3.3. SGD flux estimations

The trend with distance offshore (Fig. 2) displayed by Ra isotopes may be used to estimate the eddy diffusion coefficient (K_h) and the advection offshore (u), following an approach described by Moore (2000a) and modified by Li and Cai (2011). The equations used in this approach are given below:

$$u = \frac{L_1^2\lambda_1 - L_2^2\lambda_2}{L_2 - L_1} \quad (1)$$

$$K_h = L_2^2\lambda_2 + L_2 u = L_1^2\lambda_1 + L_1 u \quad (2)$$

where L_1 and L_2 are the inverse (1/m) of the slopes from the log-linear fit for ^{223}Ra and ^{224}Ra versus distance offshore respectively, u is the offshore advective velocity (m s^{-1}), K_h is the horizontal eddy diffusivity coefficient (m^2 s^{-1}), and λ_1 and λ_2 are the radioactive decay coefficients of the two short-lived Ra isotopes (s^{-1}). Here, ^{223}Ra and ^{224}Ra are used because their half-lives are comparable to the expected residence time of nearshore waters. This approach assumes that there are no additional inputs of the tracer beyond the coastline. Assuming shore-based Ra sources to the Palma Beach, an

299 exponential decrease offshore should be observed for the distribution of the $^{224}Ra/^{226}Ra$
300 activity ratio (AR), since ^{224}Ra decays faster than ^{226}Ra. However, this AR was constant
301 from the coastline to ~500 m offshore (Fig. 7), suggesting either that Ra inputs are
302 occurring all along the first 500 m (what would violate the initial assumption of the
303 approach) or that there is a fast mixing in this nearshore area (what would imply a
304 higher diffusion/advection in this specific region than in the rest of the bay). Thus, only
305 the samples collected beyond 500 m of the coastline are considered to obtain the
306 diffusion and advection coefficients for the entire bay. The log-linear fit of ^{223}Ra and
307 ^{224}Ra concentrations versus distance offshore allows estimating a diffusive mixing
308 coefficient (K_h) of 2.6±0.4 m^2 s^{-1} and a very low advection velocity (0.0011±0.0006 m
309 s^{-1}). This almost negligible estimated advection velocity is in good agreement with the
310 bay circulation patterns modeled by Jordi et al. (2011) that resulted in a minor net
311 offshore water current.
312 If the advection and diffusive mixing coefficients are known, the fluxes offshore of
313 any conservative material can be calculated. As advection in our system has been shown
314 to be negligible, the flux of ^{226}Ra offshore from the Palma bay can be estimated as the
315 product of the offshore ^{226}Ra concentration gradient and the Ra-derived eddy diffusivity
316 constant (K_h) (Moore, 2000a). Since all the three transects conducted perpendicular to
317 the coastline present similar ^{226}Ra patterns, they are integrated in order to obtain a value
318 for the study site. Taking the linear ^{226}Ra gradient (-9.6 ± 1.8) 10^{-3} dpm m^{-3} m^{-1} (r^2 =
319 0.817; $p < 0.001$) and assuming that the tracer was transported offshore in the 3.5 m
320 fresher surface layer, the offshore ^{226}Ra flux is 0.088 ± 0.020 dpm m^{-1} s^{-1}. The ^{226}Ra
321 flux offshore must be balanced by an input in the coastal zone, most likely SGD. Other
322 potential sources of ^{226}Ra can be neglected: surface water inputs to the bay are
323 insignificant during the dry season and ^{226}Ra release from sediments is minimal due to

its low activity in bay sands (0.85 ± 0.21 dpm g^{-1}; n=3) and long regeneration time (Beck et al., 2007b).

This estimated ^{226}Ra flux may be converted into a SGD flow by characterizing the ^{226}Ra concentration in SGD. Considering that long-lived Ra isotopes are not significantly decaying on the time scale of nearshore processes, the ^{226}Ra and ^{228}Ra concentration in SGD must accomplish the following mixing equations:

$$f_{SGD} + f_{SW} = 1 \quad (3)$$

$$^{226}Ra_{SGD} f_{SGD} + {}^{226}Ra_{SW} f_{SW} = {}^{226}Ra_{BW} \quad (4)$$

$$^{228}Ra_{SGD} f_{SGD} + {}^{228}Ra_{SW} f_{SW} = {}^{228}Ra_{BW} \quad (5)$$

where f is the fraction of SGD (SGD) and open sea water (SW) end-members in Palma Beach waters (BW), respectively, and Ra_{SGD}, Ra_{SW} and Ra_{BW} are the average concentration of ^{226}Ra and ^{228}Ra in SGD, open sea waters (^{226}Ra = 9.4 dpm 100L^{-1} and ^{228}Ra = 2.3 dpm 100L^{-1}; Moore, 2006) and Palma Beach waters (^{226}Ra =13.8 dpm 100L^{-1} and ^{228}Ra = 5.7 dpm 100L^{-1}), respectively. Given that there are more unknowns (f_{SGD}, f_{SW}, AR_{SGD} and $^{226}Ra_{SGD}$) than equations, ^{226}Ra in SGD can be only constrained by evaluating a range of ^{228}Ra concentrations. As seen from Fig. 5b, only two samples collected present ^{228}Ra and ^{226}Ra concentrations in accordance to the requirements imposed by these equations, and thus they were considered as the representative SGD end-member for Ra isotopes. Indeed, these are two porewater samples collected in the NW part of the Palma Beach, where the shallow aquifer connects with the sea (preferential groundwater flow lines in Fig 1). Using the average ^{226}Ra concentration in these two porewater samples (59 ± 2 dpm 100L^{-1}), the calculated SGD seepage flow 12.8 ± 3.0 m^3 m^{-1} d^{-1}. Assuming that diffusive groundwater discharge occurred all along the Palma Beach coastline (4400 m), the total flow to the Bay is 56000 ± 1300 m^3 d^{-1}. This value is almost three times higher than the groundwater discharge derived from the

regional hydrological balance (20000 m^3 d^{-1}; PHIB, 2008). This discrepancy likely reflects the fact that the hydrological budget takes into account only the fresh groundwater discharge, while the Ra approach also includes the recirculated seawater, which can also be an important source of terrestrial compounds to the coastal sea.

3.4. Residence time of conservative compounds

An estimation of the time that coastal conservative compounds remained in the study site (i.e. residence time) is needed to evaluate the implications of SGD-driven fluxes on the coastal ecosystem. The residence time of conservative compounds can be calculated using the variation of the activity ratios (AR) between Ra isotopes of different half-lives, based on an approach described by Moore (2000b). This approach assumes that (i) Ra is only added to coastal water in the source region, (ii) there are no losses of Ra aside from mixing and radioactive decay, (iii) Ra entering the system has a uniform AR and (iv) the open sea contains negligible concentrations of Ra. Given that Ra inputs in Palma Beach are likely occurring along the first 500 m from the shoreline (Fig 7), here we define residence time of conservative compounds as the time it takes for them to leave the study site (2000 m offshore) since they were isolated from the source area (0 – 500 m). Following the approach described by Moore (2000b), residence time of conservative compounds (T_R) can be calculated as follows:

$$T_R = \frac{\ln (AR_{2000}) - \ln (AR_{SR})}{\lambda_{224} - \lambda_{226}} \quad (6)$$

where AR_{2000} is the $^{224}Ra/^{226}Ra$ AR at 2000 m offshore (0.14 ± 0.05) and AR_{SR} is the average $^{224}Ra/^{226}Ra$ AR in the source region (0.70 ± 0.09), and λ_{224} (0.189 d^{-1}) and λ_{226} (negligible relative to λ_{224}) are the decay constants of ^{224}Ra and ^{226}Ra, respectively. Here, ^{224}Ra was selected because its half-life is appropriate for the expected residence time of the site and ^{226}Ra as a normalizing isotope because its decay is negligible and it

374 has lower relative uncertainties than ^{223}Ra. Applying Eq. 6, a residence time for
375 conservative compounds in the study site of 8.4 ± 1.9 days was obtained (Fig. 7).
376

4. DISCUSSION

4.1. Nutrient inputs through SGD

The analysis of nutrient concentrations in coastal piezometers and wells suggest that fresh groundwater is a dominant supplier of DIN to Palma Beach (Fig. 6). Porewater samples roughly fall along the mixing line between nutrient-rich fresh groundwater and nutrient-poor seawater end-members, revealing that the mixing with recirculated seawater acts mainly as a dilution agent. However, several samples lie below this conservative mixing line, likely reflecting the complex geochemical behaviour of nutrients in the subterranean estuary. The high DIN pools measured in fresh groundwater samples, largely as nitrate (~ 99 %), agree with other results reported along the island (López-Garcia and Mateos-Ruiz, 2003). These high nitrate concentrations in groundwater are mainly a consequence of intensive irrigation practices based on wastewater reuse and fertilizers use (Candela et al., 2008; López-Garcia and Mateos-Ruiz, 2003). Unlike DIN, DIP concentrations are very low in fresh groundwater (Fig. 6), which is attributed to its rapid removal from groundwater (Slomp and Van Cappellen, 2004) and a minor influence of anthropogenic inputs. The highest DIP concentrations were measured in mid-salinity porewater, most likely due to the mobilization of phosphate in the subterranean estuary by recirculated seawater (Weinstein et al., 2011).

The nutrient fluxes from SGD to the Palma Bay can be calculated by multiplying the amount of SGD derived from Ra isotopes by the concentration of nutrients in inflowing SGD (Table 1). Given that nutrients do not behave conservatively along the groundwater path and concentration in the subterranean estuary are extremely variable, the estimation of the nutrient concentration in the actual SGD end-member becomes particularly difficult (see discussion on nutrient end-member selection in Santos et al.

(2008) and Knee et al. (2010)). To provide a reasonable characterization of nutrient concentrations in SGD a large number of samples along the study site was used, focusing on groundwater sampled just before discharging and in the upper 2 m of the subterranean estuary, considered the most permeable layer where most biogeochemical reactions are occurring (Santos et al., 2008). The range comprised between the 1st and 3rd quartiles of the set of nutrient concentration in groundwater (wells and piezometers; n = 23) was used as a reasonable upper and lower estimate of nutrients in discharging SGD (Table 1). The dissolved nutrient concentrations in these end-members spanned a wide range (e.g. up to two orders of magnitude for DIN; Table 1) and thus result in SGD-driven nutrient fluxes with large uncertainties (Table 1). The contribution of seawater was removed to calculate the nutrient flux derived from SGD (Santos et al., 2008). The resulting flux of nutrients into Palma Beach ranges from 100 to 10000 and from 3 to 31 mmol m^{-1} d^{-1} for DIN and DIP, respectively, with a median flux of 1900 mmol m^{-1} d^{-1} of DIN and 16 mmol m^{-1} d^{-1} of DIP. DIN fluxes are in the upper range of values reported in different coastal areas (Slomp and Van Cappellen (2004) for a compilation), mainly as a consequence of the high DIN concentrations in groundwater (Candela et al., 2008; López-Garcia and Mateos-Ruiz, 2003). Conversely, DIP fluxes are low, as dissolved phosphate is rapidly removed from groundwater through sorption to Fe-oxides or co-precipitation with metal into mineral phases (Slomp and Van Cappellen, 2004). This contrasting behavior translates into ratios of dissolved inorganic N:P in inflowing SGD of 160:1, much higher than the requirements by phytoplankton growth (Redfield N:P ratio of 16:1). Similar ratios in inflowing SGD have been reported in other Mediterranean settings (Garcia-Solsona et al., 2009; 2010). Thus, this SGD input may contribute to P limitation in the area, what is a common situation in the Mediterranean Sea (e.g. Díaz et al., 2001).

427 The significance of SGD as a source of nutrients into nearshore waters of Palma
428 Beach can be assessed through the comparison of the SGD-derived nutrient inventory
429 (i.e. nutrient flux from SGD multiplied by the residence time obtained from Ra
430 isotopes) and the excess inventory of nutrients in the study site (i.e. average nutrient
431 concentration in nearshore water minus nutrient concentration offshore, multiplied by
432 the volume of the study site). Notice that the study site must be described by the same
433 boundaries used when SGD is estimated (3.5 m depth and 2000 m width) and that
434 constant nutrient concentrations are assumed for the 3.5 m surface layer. This
435 qualitative comparison reveals that the amount of DIN and DIP supplied by SGD would
436 account for 120% and 40%, respectively, of the excess pools of these nutrients
437 measured in nearshore waters (Fig. 8). Although this comparison does not take into
438 account the complex cycling of nutrients in seawater (e.g. transformation, removal or
439 release of nutrients due to biological processes or fluxes from/to bottom sediments), it
440 still provides valuable information on the relevance of SGD as a source of nutrients to
441 the study site. In doing so, we found that SGD is a major source of DIN and can also
442 contribute substantial amounts of DIP to nearshore waters of this Mediterranean bay.
443 Indeed, strong offshore gradients of DIN and, to a lesser extent, DIP concentration,
444 were measured in seawater (Fig. 3), which provides independent evidence of the
445 significant role of SGD as a source of these compounds to the sea.
446
447 **4.2. Trace metal inputs through SGD**
448 Biogeochemical processes occurring at the subterranean estuary commonly result in
449 non-conservative behavior for trace metals in groundwater (Beck et al., 2010). The
450 distribution of trace metals in piezometers and wells relative to salinities (Fig. 6) could
451 provide some insight about their relative sources and behavior in the subterranean

estuary. Dissolved Cu and Zn show higher concentrations in fresh groundwater (concentrations in wells up to 1 and 2 orders of magnitude, respectively, higher than in seawater) and their removal from solution may be controlled by dilution, redox conditions and by the dissolution or precipitation of Mn oxides (Beck et al., 2010; Charette and Sholkovitz, 2006). Unfortunately, neither Mn concentration nor oxido-reductive potential were monitored in this study. On the other side, distribution of dissolved Mo show higher concentration in high-salinity waters. Indeed, when normalizing Mo concentrations to salinity, only few samples have higher concentrations than those contributed by seawater, revealing that groundwater is not a source of this metal. The other dissolved metals analyzed in this study (Fe, Ni and Pb) are markedly enriched in porewaters compared to fresh groundwater from wells and seawater, most likely as a consequence of the geochemical processes occurring at the subterranean estuary. As an example, dissolved Fe shows low levels in both fresh groundwater and seawater, but it is highly enriched (1 to 3 orders of magnitude) in the high-salinity piezometers. Similar enrichments of dissolved Fe in the subterranean estuary have been attributed to Fe-oxide reduction due to elevated dissolved organic carbon (DOC) concentrations at the freshwater-saltwater boundary (Roy et al., 2010; Snyder et al., 2004). Moreover, Fe-oxides may be reduced as pore water is likely anoxic, what prevents Fe-oxides precipitation and promotes their release to the pore waters (Roy et al., 2010).

The behavior of these trace metals within the subterranean estuary must be taken into account when determining the SGD-driven metal fluxes (Beck et al., 2007a). As detailed earlier, the range comprised between the 1st and 3rd quartiles of the set of metal concentration in groundwater (including wells and piezometers; n = 23) are considered the best characterization of the metal concentration in SGD (Table 1). These metal

477 concentration ranges are then multiplied by the Ra-derived groundwater discharge and
478 the metal contribution from seawater is subtracted, to obtain the SGD-driven trace metal
479 fluxes to the Palma Beach (Table 1). Although subject to large uncertainties due to the
480 measured variability and complex distribution patterns of trace metal in the
481 subterranean estuary (Fig. 6; Table 1), these estimated fluxes provide valuable
482 information, as this is the first study in the Mediterranean Sea where trace metal fluxes
483 from SGD have been estimated. As expected from the concentration of trace metals in
484 porewaters, the flux of dissolved Fe from SGD (median flux of 4.1 mmol m^{-1} d^{-1}) is 1 to
485 3 fold higher than fluxes of other elements (Table 1). All the SGD-driven fluxes of trace
486 metals calculated here are considerably lower (~1 order of magnitude) than fluxes
487 reported in coastal areas worldwide (e.g. Beck et al., 2007a; Charette and Sholkovitz,
488 2006; Jeong et al., 2012), mainly because the magnitude of the SGD in all the other
489 settings is 1-2 orders of magnitude higher than in Palma Bay.
490 In order to evaluate the significance of the SGD-driven metal fluxes to the coastal
491 seawater pools, the contribution of metals from SGD can be compared with the excess
492 metal inventory measured in the study site (estimated as explained for nutrients; Section
493 4.1.). The SGD-driven inventory of Fe into Palma Beach represents 0.2 – 9 times
494 (median of 1.9) the inventory of dissolved Fe actually measured in the bay, indicating
495 that SGD is a significant source of dissolved Fe into the study site (Fig. 8)". It may also
496 suggest a significant removal of dissolved Fe due to precipitation, scavenging by
497 particles or biological uptake, as this comparison does not take into account other
498 sources or sinks of trace metals. In contrast, the estimated SGD-driven inventories for
499 all the other measured trace metals are 1-2 orders of magnitude lower than the measured
500 inventories of these metals in seawater (Fig. 8). Similar differences among trace metals
501 were reported in a volcanic island (Jeju Island, Korea) by Jeong et al. (2012). These

502 authors concluded that SGD is particularly important for the transport of major elements
503 of the earth's crust, such as Fe and Al, to the coastal waters, where they exist at trace
504 levels. Indeed, the distribution of trace metals in the entire Palma Bay (Fig. 4) shows a
505 marked Fe enrichment in nearshore samples from Palma Beach, where the shallow
506 aquifer is directly connected to the sea and where the main SGD inputs are expected.
507 This provides significant independent evidence of the relevance of SGD as a Fe source.
508 This pattern is not observed for all the other trace metals (Ni, Cu, Zn, Mo and Pb; Fig.
509 4), agreeing well with the comparison of SGD-driven and measured inventories derived
510 in this study (Fig. 8). It is worth noticing that there is an important source of Cu, Zn and
511 Pb to nearshore waters from the NW part of the Palma Bay, close to the city of Palma
512 and the harbor. The high concentration of Cu and Zn measured there could be related to
513 the maritime traffic, as boating traffic is considered an important source of Cu and Zn to
514 the coastal environments (Garcia-Orellana et al., 2011; Matthiessen et al., 1999).
515 Atmospheric inputs are considered the major supplier of dissolved metals to
516 Mediterranean surface waters on a basin-wide scale, mainly due to Saharan dust
517 deposition events (Bonnet and Guieu, 2006; Guerzoni et al., 1999). Focusing on coastal
518 areas, a comparison between atmospheric inputs of dissolved Fe in the Western
519 Mediterranean during summer time (0.3 μmol m^{-2} d^{-1}; Bonnet and Guieu, 2006) and the
520 Fe supply from SGD obtained in this work (2.0 μmol m^{-2} d^{-1}; Table 1) illustrates the
521 potential significance of SGD as a relevant source of dissolved Fe to Mediterranean
522 coastal areas. SGD could represent a major source of trace metals to the coastal sea and
523 needs to be considered in future studies of trace metal cycling in the coastal
524 Mediterranean Sea.
525
526 **4.3. Conclusions and ecological implications of SGD**

527 The results obtained in this study reveal that the fluxes of chemical constituents,
528 especially nutrients and dissolved Fe, associated to SGD play a significant role on the
529 coastal budgets of these elements in Palma Beach and may also have a critical impact
530 on the primary productivity. In fact, an onshore-offshore gradients of phytoplankton
531 biomass (Fig. 3) and strong linear relationships between Chl*a* concentrations and Ra
532 activities in coastal water samples ($r^2 > 0.7$; $p < 0.001$; Fig. 9) suggest a connection
533 between phytoplankton biomass and SGD. The high phytoplankton biomass measured
534 in the region thus seems reasonably sustained by the inputs of chemical constituents
535 derived from SGD. A significant impact of SGD on the coastal productivity of Mallorca
536 Island has been previously suggested by Basterretxea et al. (2010). Further studies (e.g.
537 in situ groundwater addition experiments such as those conducted by Garcés et al.,
538 2011) are needed in order to more thoroughly assess the role of SGD on phytoplankton
539 growth. As the bioproductivity in the Mediterranean Sea is largely limited by phosphate
540 availability (e.g. Díaz et al., 2001), inputs of DIP through SGD may be especially
541 important. However, the high N:P ratio in SGD actually seems to promote P limitation.
542 It is worth noting that SGD inputs of dissolved Fe are also relevant because other major
543 Fe inputs in the study area are nonexistent and dissolved Fe is often a limiting bioactive
544 element for many primary producers and marine organisms, such as *Posidonia oceanica*
545 (Tovar-Sánchez et al. 2010; Marbà et al., 2007) and *Synechoccocus* (Garcés et al.,
546 2011).
547 Inputs of nutrients and other micronutrients via SGD may play an important role in
548 the regulation of nearshore phytoplankton communities, especially in oligotrophic areas
549 such as the Mediterranean Sea. The SGD-driven inputs of terrestrial compounds,
550 together with physical factors (such as summer calm conditions and bay
551 geomorphology), provide an ideal environment for bloom outbreaks and biomass

552 accumulation in nearshore waters (Basterretxea et al., 2007). SGD could thus contribute
553 explaining the high frequency of Mediterranean coastal blooms, an emerging problem
554 with significant ecological and economical implications.
555

ACKNOWLEDGEMENTS

This project has been funded partially by the Spanish Government projects EDASE (ref. CGL2008-00047/BTE) and GRADIENTS (CTM2012-39476-C02-01). V.R. acknowledges financial support through a PhD fellowship (AP2008-03044) from MICINN (Spain). Support from a post-doctoral fellowship to E.G-S. (EX2009-0651; Plan Nacional de I-D+i 2008-2011, Spain) is acknowledged. Support for the research of P.M. was received through the prize ICREA Academia, funded by the Generalitat de Catalunya. The manuscript was improved by comments from A. Paytan and three anonymous reviewers. We would like to gratefully acknowledge our colleagues at the Laboratori de Radioactivitat Ambiental (UAB) and the IMEDEA for their help and assistance during field and lab work.

568
569 **REFERENCES**

570 Basterretxea G, Garcés E, Jordi A, Angles S, Masó M. Modulation of nearshore
571 blooms by growth rate and water renewal. Mar Ecol Prog Ser 2007; 352:53-65.
572 Basterretxea G, Tovar-Sanchez A, Beck AJ, Masqué P, Bokuniewicz HJ, Coffey R,
573 Duarte CM, Garcia-Orellana J, Garcia-Solsona E, Martinez-Ribes L, Vaquer R, Sañudo-
574 Wilhelmy SA. Submarine Groundwater Discharge to the Coastal Environment of a
575 Mediterranean Island (Majorca, Spain): Ecosystem and Biogeochemical Significance.
576 Ecosystems 2010;13:629-643.
577 Beck AJ, Tsukamoto Y, Tovar-Sánchez A, Huerta-Diaz M, Bokuniewicz HJ and
578 Sañudo-Wilhelmy SA. Importance of geochemical transformations in determining
579 submarine groundwater discharge-derived trace metal and nutrient fluxes. Appl
580 Geochem 2007a;22:477-490.
581 Beck AJ, Rapaglia J, Cochran JK, Bokuniewicz HJ. Radium mass-balance in
582 Jamaica Bay, NY: Evidence for a substantial flux of submarine groundwater. Mar Chem
583 2007b;106:419-441.
584 Beck AJ, Cochran JK, Sañudo-Wilhelmy SA. The distribution and speciation of
585 dissolved trace metals in a shallow subterranean estuary. Mar Chem 2010;121:145-156.
586 Bonnet S, Guieu C. Atmospheric forcing on the annual iron cycle in the western
587 Mediterranean Sea: A 1-year survey. J Geophys Res 2006;111: C09010,
588 doi:10.1029/2005JC003213.
589 Burnett WC, Bokuniewicz H, Huettel M, Moore WS and Taniguchi M.
590 Groundwater and porewater inputs to the coastal zone. Biogeochemistry 2003;66: 3-33.
591 Cai WJ, Wang YC, Krest J, Moore WS. The geochemistry of dissolved inorganic
592 carbon in a surficial groundwater aquifer in North Inlet, South Carolina, and the carbon
593 fluxes to the coastal ocean. Geochim Cosmochim Ac 2003;67:631-639.
594 Candela L, Wallis KJ, Mateos RM. Non-point pollution of groundwater from
595 agricultural activities in Mediterranean Spain: Balearic Islands case study. Environ Geol
596 2008;54:587-95.
597 Charette MA, Sholkovitz ER. Trace element cycling in a subterranean estuary: Part
598 2. Geochemistry of the pore water. Geochim Cosmochim Ac 2006;70:811–826.
599 Díaz F, Raimbault P, Boudiellal B, Garcia N, Moutin T. Early spring phosphorous
600 limitation of primary productivity in a NW Mediterranean coastal zone (Gulf of Lions).
601 Mar Ecol-Prog Ser 2001;211:51-62.

602 Garcés E, Basterretxea G, Tovar-Sánchez A. Changes in microbial communities in
603 response to submarine groundwater input. Mar Ecol-Prog Ser 2011;438:47-58.
604 Garcia-Orellana J, Cañas L, Masqué P, Obrador B, Olid C, Pretus J. Chronological
605 reconstruction of metal contamination in the Port of Maó (Minorca, Spain). Mar Pollut
606 Bull 2011;62:1632-1640
607 Garcia-Solsona E, Garcia-Orellana J, Masqué P, Dulaiova H. Uncertainties
608 associated with ^{223}Ra and ^{224}Ra measurements in water via Delayed Coincidence
609 Counter (RaDeCC). Mar Chem 2008;109:198-219.
610 Garcia-Solsona E, Garcia-Orellana J, Masqué P, Garcés E, Radakovitch O, Mayer
611 A, Estradé S, Basterretxea G. An assessment of karstic submarine groundwater and
612 associated nutrient discharge to a Mediterranean coastal area (Balearic Islands, Spain)
613 using radium isotopes. Biogeochemistry 2009; 97:211–29.
614 Garcia-Solsona E, Garcia-Orellana J, Rodellas V, Mejías M, Ballesteros BJ,
615 Domínguez JA. Groundwater and nutrient discharge through karstic coastal springs
616 (Castelló, Spain). Biogeosciences 2010;7:2625-2638.
617 Grasshoff K, Ehrhardt M, Kremling K, Almgreen T. Methods of seawater analysis.
618 Wiley; 1983.
619 Guerzoni S, Chester R, Dulac F, Herut B, Loÿe-Pilot M-D, Measures C, Migon C,
620 Molinaroli E, Moulin C, Rossini P, Saydam C, Soudine A, Ziveri P. The role of
621 atmospheric deposition in the biogeochemistry of the Mediterranean Sea. Prog
622 Oceanogr 1999;44:147-190.
623 Hancock GJ, Murray AS. Source and distribution of dissolved radium in the Bega
624 River estuary, Southeastern Australia. Earth Planet Sci Lett 1996;138:45-155.
625 Howarth R, Anderson D, Cloern C, Elfring C, Hopkinson C, Lapointe B, Malone T,
626 Marcus N, Mcglathery K, Sharpley AN. Nutrient pollution of coastal rivers, bays, and
627 seas. Issues in Ecology 2000;7:1-15.
628 Jeong J, Kim G, Han S. Influence of trace element fluxes from submarine
629 groundwater discharge (SGD) on their inventories in coastal waters of volcanic islands,
630 Jeju, Korea. Appl Geochem 2012;27:37-43.
631 Jordi A, Basterretxea G, Wang DP. Local versus remote wind effects on the coastal
632 circulation of a microtidal bay in the Mediterranean Sea. J Marine Syst 2011;88:312-
633 322.
634 Knee KL, Street JH, Grossman EE, Boehm AB, Paytan A. Nutrient inputs to the
635 coastal ocean from submarine groundwater discharge in a groundwater-dominated

636 system: Relation to land use (Kona coast, Hawaii, USA). Limnol Oceanogr
637 2010;55;1105-1122.
638 Knee KL, Garcia-Solsona E, Garcia-Orellana J, Boehm AB, Paytan A. Using
639 radium isotopes to characterize water ages and coastal mixing rates: A sensitivity
640 analysis. Limnol Oceanogr: Methods 20011;9;380-395.
641 Lee YW, Kim G, Lim WA, Hwang DW. A relationship between submarine
642 groundwater-borne nutrients traced by Ra isotopes and the intensity of dinoflagellate
643 red-tides occurring in the southern sea of Korea. Limnol Oceanogr 2010;55:1-10.
644 Li C, Cai WJ. On the calculation of eddy diffusivity in the shelf water from radium
645 isotopes: High sensitivity to advection. J Marine Syst 2011;86:28-33.
646 Li L, Barry D, Stagnitti F, Parlange JP. Submarine groundwater discharge and
647 associated chemical input to a coastal sea. Water Resour Res 1999; 35:3253-3259.
648 López-García JM, Mateos-Ruiz RM. La intrusión marina en los acuíferos costeros
649 de la Isla de Mallorca. Tecnología de la Intrusión de Agua de Mar en Acuíferos
650 Costeros: Países Mediterráneos. Publicaciones del Instituto Geológico y Mineros de
651 España. Serie: Hidrogeología y Aguas Subterráneas nº8. Tomo I. 383-392. ISBN: 84-
652 7840–470–8; 2003. *[In Spanish]*
653 Marbà N, Calleja ML, Duarte CM, Alvarez E, Díaz-Almela E, Holmer M. Iron
654 additions reduce sulfide intrusion and reverse seagrass (Posidonia oceanica) decline in
655 carbonate sediments. Ecosystems 2007;10:745-756.
656 Matthiessen P, Reed J, Johnson M. Sources and potential effects of Copper and
657 Zinc concentrations in the estuarine waters of Essex and Suffolk, United Kingdom. Mar
658 Pollut Bull 1999;38:908-920.
659 Moore WS. The subterranean estuary: a reaction zone of ground water and sea
660 water. Mar Chem 1999;65:111-125.
661 Moore WS. Determining coastal mixing rates using radium isotopes. Cont Shelf
662 Res 2000a; 20: 1993-2007.
663 Moore WS. Ages of continental shelf waters determined from Ra-223 and Ra-224. J
664 Geophys Res-Oceans 2000b;105:22117-22122.
665 Moore WS. Radium isotopes as tracers of submarine groundwater discharge in
666 Sicily. Cont Shelf Res 2006;8:852-861.
667 Moore WS, Reid DF. Extraction of Radium from Natural Waters Using
668 Manganese-Impregnated Acrylic Fibers. J Geophys Res 1973;79:8880-8886.
669 Moore WS, Arnold R. Measurement of ^{223}Ra and ^{224}Ra in coastal waters using a

delayed coincidence counter. J Geophys Res 1996;101:1321-1329.

Nielsen KA, Clemmensen LB, Fornós JJ. Middle Pleistocene magnetostratigraphy and susceptibility stratigraphy: data from a carbonate aeolian system, Mallorca, Western Mediterranean. Quat Sci Rev 2004;23:1733–56.

Parsons TR, Maita Y, Lalli CM. A manual of chemical and biological methods for seawater analysis. Oxford, UK: Pergamon Press; 1984.

PHIB. Propuesta del Plan Hidrológico de la Demarcación de Baleares. Consellería de Medi Ambient. Govern de las Illes Balears; 2008.

Rodellas V, Garcia-Orellana J, Garcia-Solsona E, Masqué P, Domínguez JA, Ballesteros BJ, Mejías M, Zarroca M, 2012. Quantifying groundwater discharge from diferent sources into a Mediterranean by using ^{222}Rn and Ra isotopes. J Hydrol 466-467, 11-22.

Roy M, Martin JB, Cherrier J, Cable JE, Smith CG. Influence of sea level rise on iron diagenesis in an east Florida subterranean estuary. Geochim Cosmochim Ac 2010;74:5560-5573.

Santos IR, Burnett WC, Chanton J, Mwashote B, Suryaputra IGNA, Dittmar T. Nutrient biogeochemistry in a Gulf of Mexico subterranean estuary and groundwater derived fluxes to the coastal ocean. Limnol Oceanogr 2008;53;705-718.

Shellenbarger GG, Monismith SG, Genin A, Paytan A. The importance of submarine groundwater discharge to the nearshore nutrient supply in the Gulf of Aqaba (Israel). Limnol Oceanogr 2006;51:1876-1886.

Slomp CP, Van Cappellen P. Nutrient inputs to the coastal ocean through submarine groundwater discharge: controls and potential impact. J Hydrol 2004;295: 64-86.

Snyder M, Taillefert M, Ruppel C. Redox zonation at the saline-influenced boundaries of a permeable surficial aquifer: effects of physical forcing on the biogeochemical cycling of iron and manganese. J Hydrol 2004;296:164-178.

Sun Y, Torgersen T. The effects of water content and Mn-fiber surface conditions on ^{224}Ra measurement by ^{220}Rn emanation. Mar Chem 1998;62:299-306.

Tovar-Sánchez A. Sampling Approaches for Trace Element Determination in Seawater. Comprehensive Sampling and Sample Preparation. In: Comprehensive Sampling and Sample preparation. Analytical Techniques for Scientists. Volume 1: Sampling theory and Methodology. doi: 10.1016/B978-0-12-381373-2.00017-X; 2012. p. 317–334.

Tovar-Sánchez A, Serón J, Marbà N, Arrieta JM, Duarte CM. Long-term records of trace metal composition of Western Mediterranean seagrass (Posidonia oceanica) meadows: natural and anthropogenic contribution. J Geophys Res: Biogeosci 2010; 115: G02006, doi:10.1029/2009JG001076.

UNESCO. Submarine groundwater discharge. Management implications, measurements and effects. IHP-VI, Series on groundwater 5. IOC manuals and guides 44. ISBN 92-9220-006-2; 2004.

Valiela I, Costa J, Foreman K, Teal JM, Howes B, Aubrey D. Transport of ground-borne nutrients from watersheds and their effects on coastal waters. Biodegradation 1990;10:177-197.

Weinstein Y, Yechieli Y, Shalem Y, Burnett WC, Swarzenski PW, Herut B. What Is the Role of Fresh Groundwater and Recirculated Seawater in Conveying Nutrients to the Coastal Ocean? Environ Sci Technol 2011;45:5195-5200.

Weinstein Y, Less G, Kafri U, Herut B. Submarine groundwater discharge in the southeastern Mediterranean (Israel). Radioact Environ 2006;8:360-72.

Windom HL, Moore WS, Niencheski LF, Jahnke RA. Submarine groundwater discharge: a large, previously unrecognized source of dissolved iron to the South Atlantic Ocean. Mar Chem 2006;102:252-266.

TABLES

Table 1. Average concentrations of nutrients (3 transects of 7 samples each one) and trace metal (n=9) in Palma Beach waters. The concentration of nutrients and trace metals in SGD is obtained from both the median and the range comprised between the 1st (Q1) and 3rd (Q3) quartiles of the set of concentrations in groundwater (wells and piezometers; n = 23). The SGD-driven flux of nutrients and trace metals normalized by shore length is estimated from both the median concentration of those compounds in SGD and the range Q1 – Q3. The SGD-driven flux of nutrients and trace metals into the entire bay and normalized by the area of the study site are also shown.

			NUTRIENTS			TRACE METALS					
			DIN	**DIP**		**Fe**	**Ni**	**Cu**	**Zn**	**Mo**	**Pb**
Seawater concentration	Mean	$\mu mol \cdot L^{-1}$	2.0	0.05	$nmol \cdot L^{-1}$	4.9	4.9	10	7	140	0.37
	SD		0.4	0.02		1.0	0.9	3	2	30	0.04
SGD concentration	Median	$\mu mol \cdot L^{-1}$	150	1.3	$nmol \cdot L^{-1}$	320	38	30	73	49	0.69
	(Q1 - Q3)		7 - 810	0.3 - 2.5		40 - 1600	12 - 53	10 - 46	12 - 120	12 - 92	0.14 - 1.0
SGD-driven flux	Median	$mmol \cdot m^{-1} \cdot d^{-1}$	1900	16	$mmol \cdot m^{-1} \cdot d^{-1}$	4.1	0.45	0.32	0.89	0	0.007
	(Q1 - Q3)		80 - 10000	3 - 31		0.4 - 20	0.13 - 0.65	0.07 - 0.53	0.1 - 1.4	0 – 0.37	0 - 0.011
	Median	$mol \cdot d^{-1}$	8500	71	$mol \cdot d^{-1}$	18	2.0	1.4	3.9	0	0.029
	Median	$\mu mol \cdot m^{-2} \cdot d^{-1}$	970	8.1	$nmol \cdot m^{-2} \cdot d^{-1}$	2000	230	160	450	0	3.3

730 **FIGURES**

731 **Figure 1.** a) The study area is located at the southeastern part of Majorca Island
732 (Balearic Islands), at the Western Mediterranean Sea. b) The hydrological formations of
733 Palma Basin are represented based on Nielsen et al. (2004) and the preferential
734 groundwater flow lines are also indicated. The location of the study site (Palma Beach),
735 at the south-east of Palma Bay, is also highlighted. c) Sampling stations in Palma Beach
736 on summer 2010. Stations include groundwater from wells (white squares), porewater
737 from piezometers (dark grey triangles) and beach seawater (grey circles). Trace metal
738 samples in beach seawater were collected in those stations highlighted with dark grey.

739 **Figure 2.** Ra activities in surface nearshore waters of Palma Beach plotted against
740 distance offshore, for all the three transects. The grey area represents the Ra activity of
741 the offshore sample with its associated uncertainty.

742 **Figure 3**. Nutrient (DIN and DIP) and Chl*a* concentrations in nearshore Palma
743 Beach waters as a function of distance offshore, for all the three transects. The grey area
744 represents the nutrient and Chl*a* concentrations measured at the offshore station.

745 **Figure 4**. Concentrations of dissolved (<0.22 μm) Fe, Ni, Cu, Zn, Mo and Pb
746 measured in surface waters from the entire Palma Bay in a previous survey conducted in
747 summer 2009. The range of concentrations for each metal is indicated in parentheses.

748 **Figure 5**. (a) ^{224}Ra vs ^{223}Ra and (b) ^{228}Ra vs ^{226}Ra activities in the potential SGD
749 end-members (groundwater from wells and piezometers). The average concentrations of
750 Ra isotopes measured in Palma Beach waters are also shown. The dashed-line in (a)
751 represents the best linear fit to the ^{224}Ra vs ^{223}Ra activities in porewaters. In (b), the
752 dashed line represents the constraint in ^{228}Ra and ^{226}Ra concentrations in inflowing SGD
753 obtained from Eq 3-5. This line is used to select those samples used as SGD end-
754 member for Ra isotopes.

Figure 6. Salinity distribution of nutrients (DIN and DIP; μmol L^{-1}) and dissolved metals (Fe, Ni, Cu, Zn, Mo and Pb; nmol L^{-1}) in groundwater from wells (grey circles) and piezometers (black triangles). The dashed line and the shadowed area, respectively, represent the median and the range comprised between the 1st and the 3rd quartiles of the set of groundwater concentrations. The averaged concentration of Palma Beach waters is also included for comparison (white diamond).

Figure 7. $^{224}Ra/^{226}Ra$ AR plotted against distance offshore. The three transects offshore were integrated in one as all of them present similar activities and distribution. The dashed line and the shadowed area, respectively, represent the average AR and the standard deviation (1σ) of the samples collected within the first 500 m from the shoreline, values used to estimate the residence time of conservative compounds in the study site.

Figure 8. Ratio of SGD-driven inventories of dissolved major nutrients and trace metals (SGD) to the inventories actually measured in seawater (SW). SGD-driven inventories are obtained from the median of all the concentrations in groundwater with lower and upper limits being the 1st and the 3rd quartiles.

Figure 9. Relations between Chl*a* and (a) ^{224}Ra and (b) ^{223}Ra. The dashed line represents the best linear fit to the data.

774 **FIGURE 1**

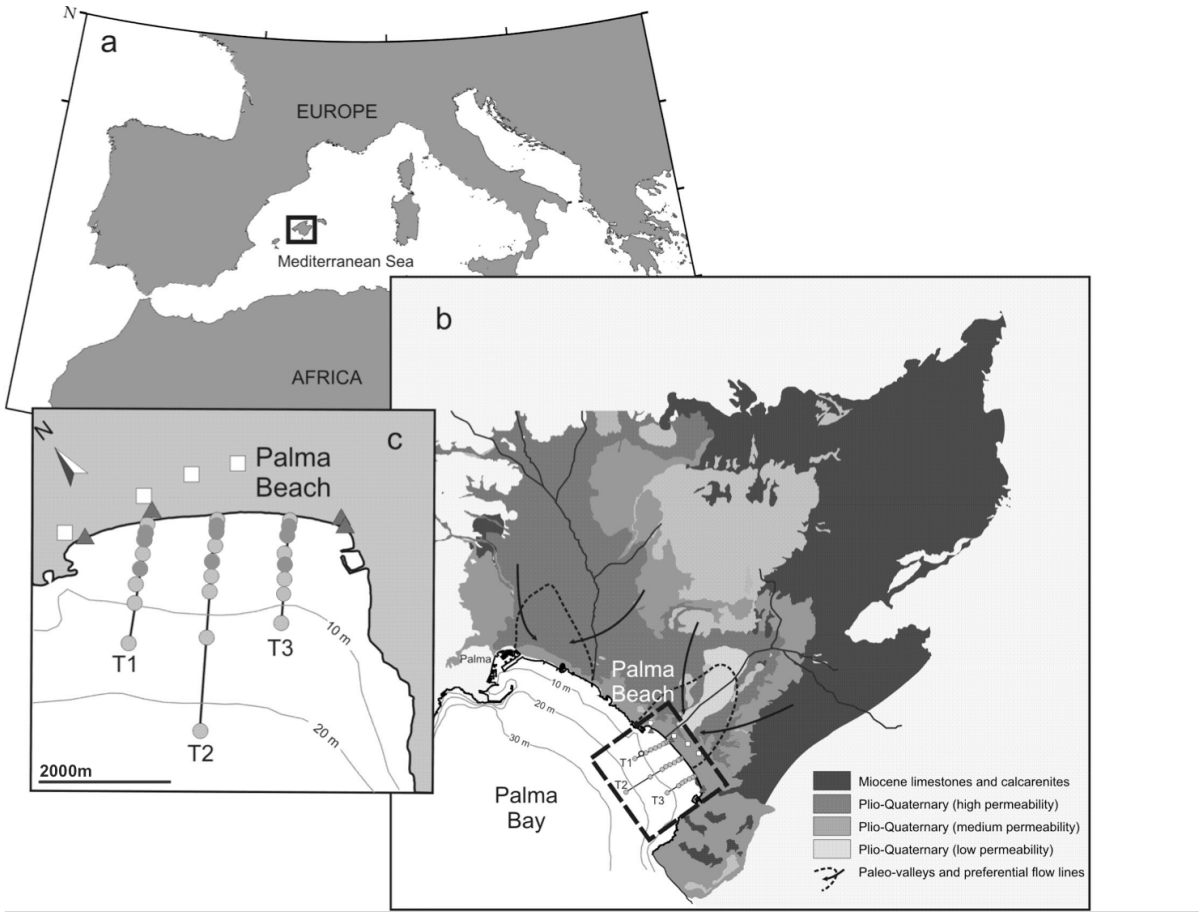

775

776

777 **FIGURE 2**

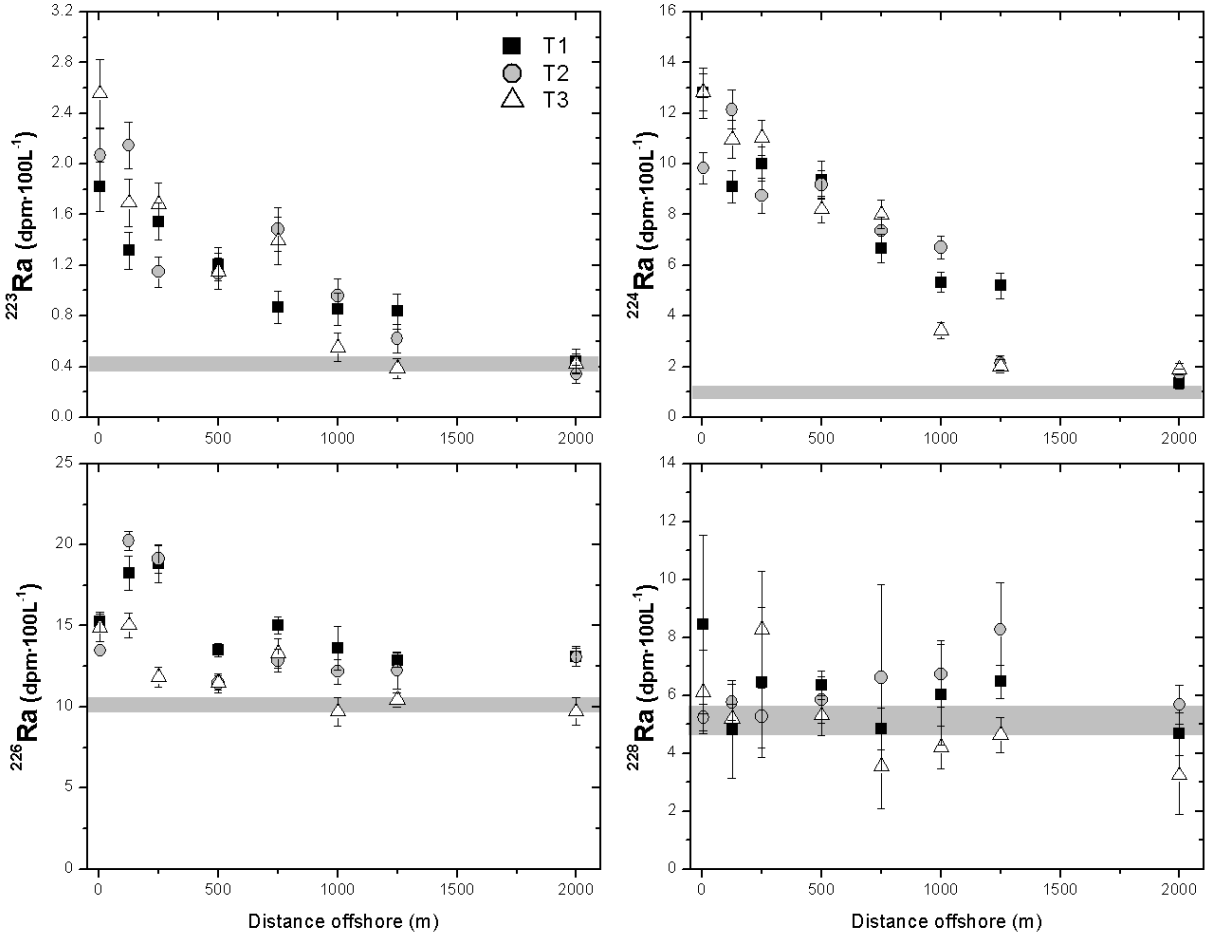

778

779

780 **FIGURE 3**

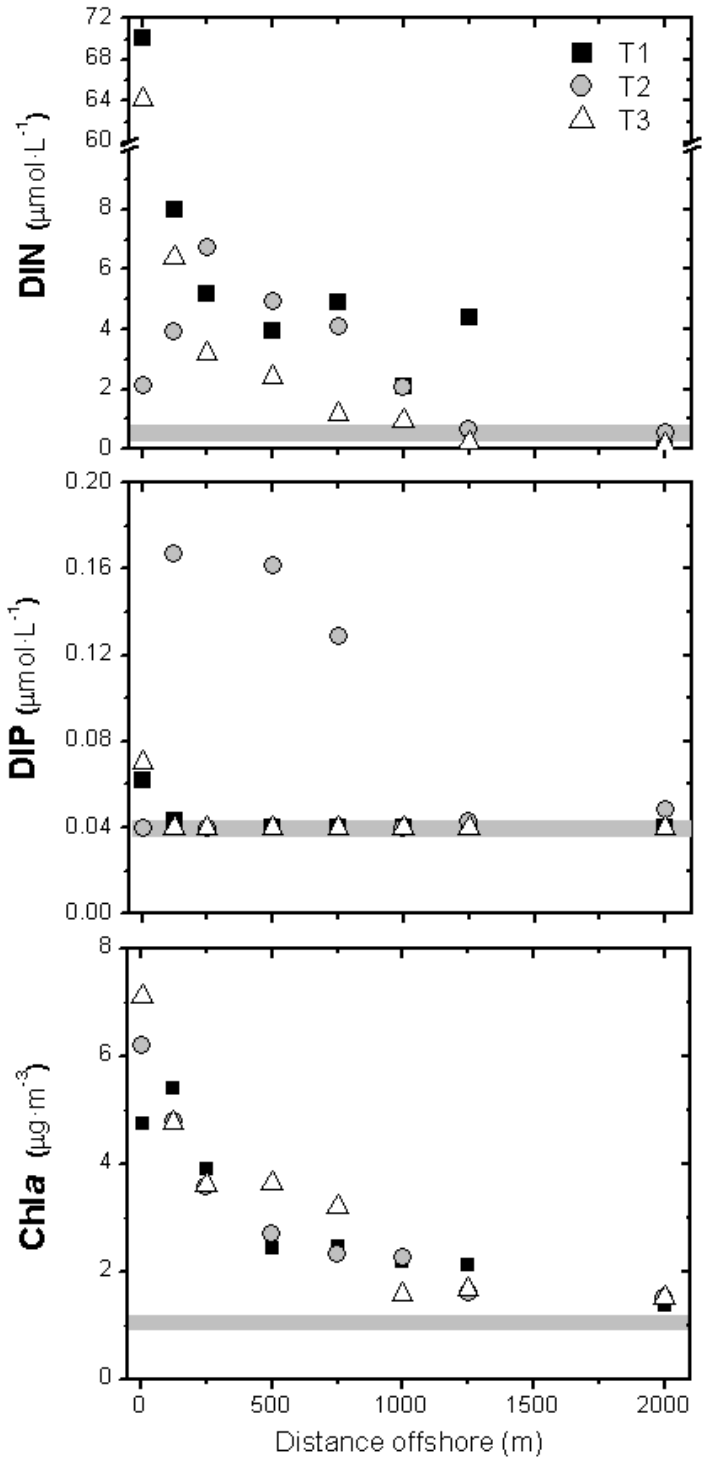

781

782

783 **FIGURE 4**

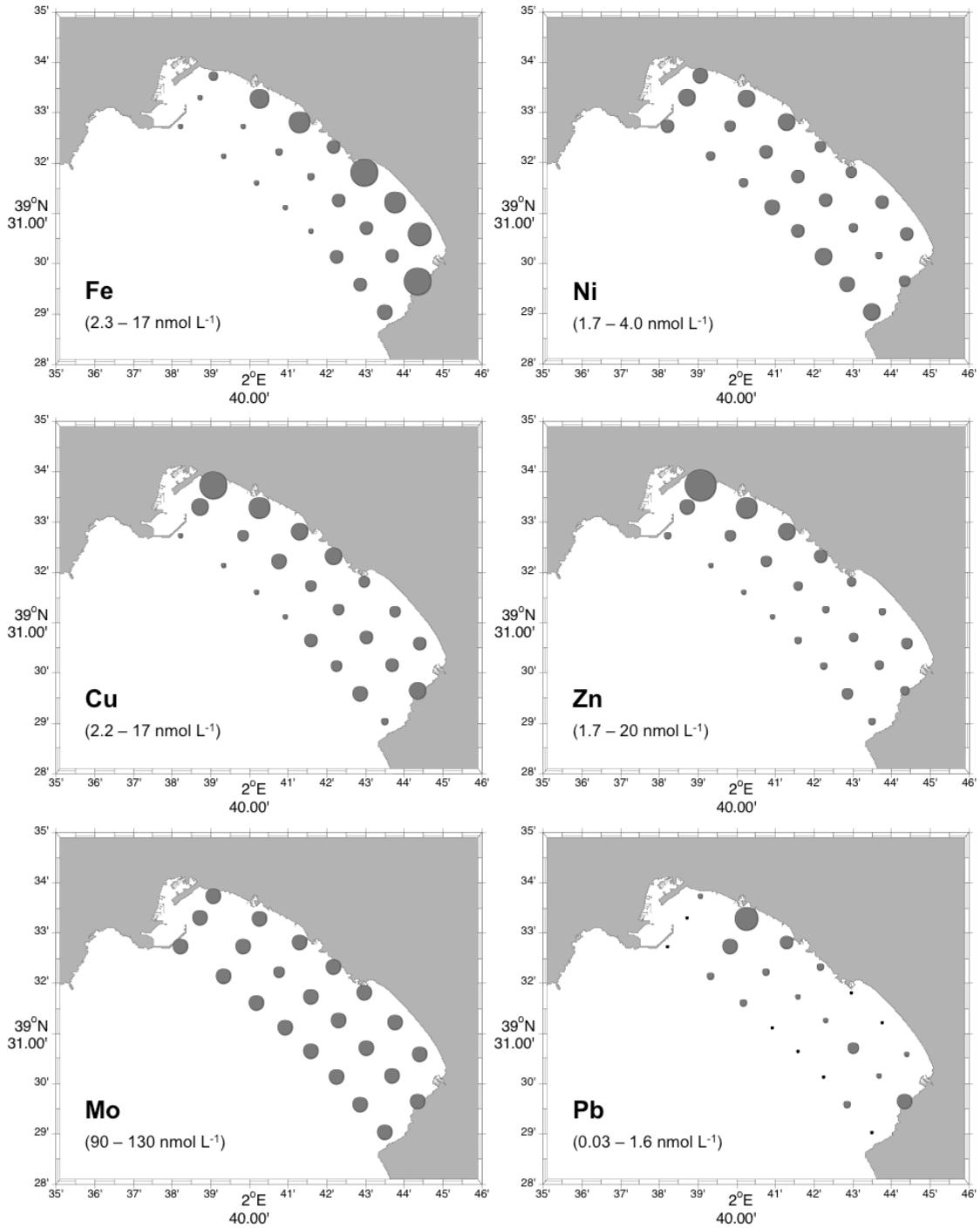

784

785

786 **FIGURE 5**

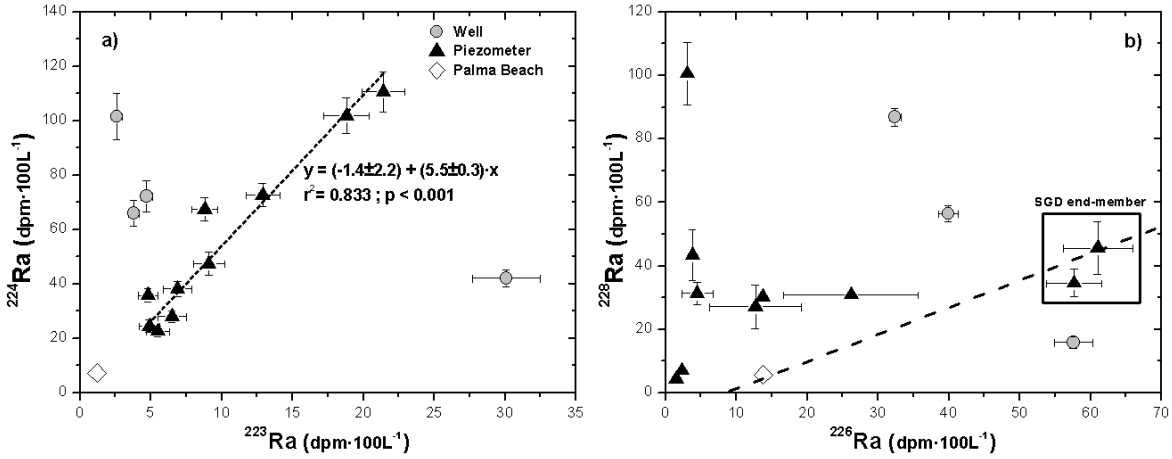

787

788

789 **FIGURE 6**

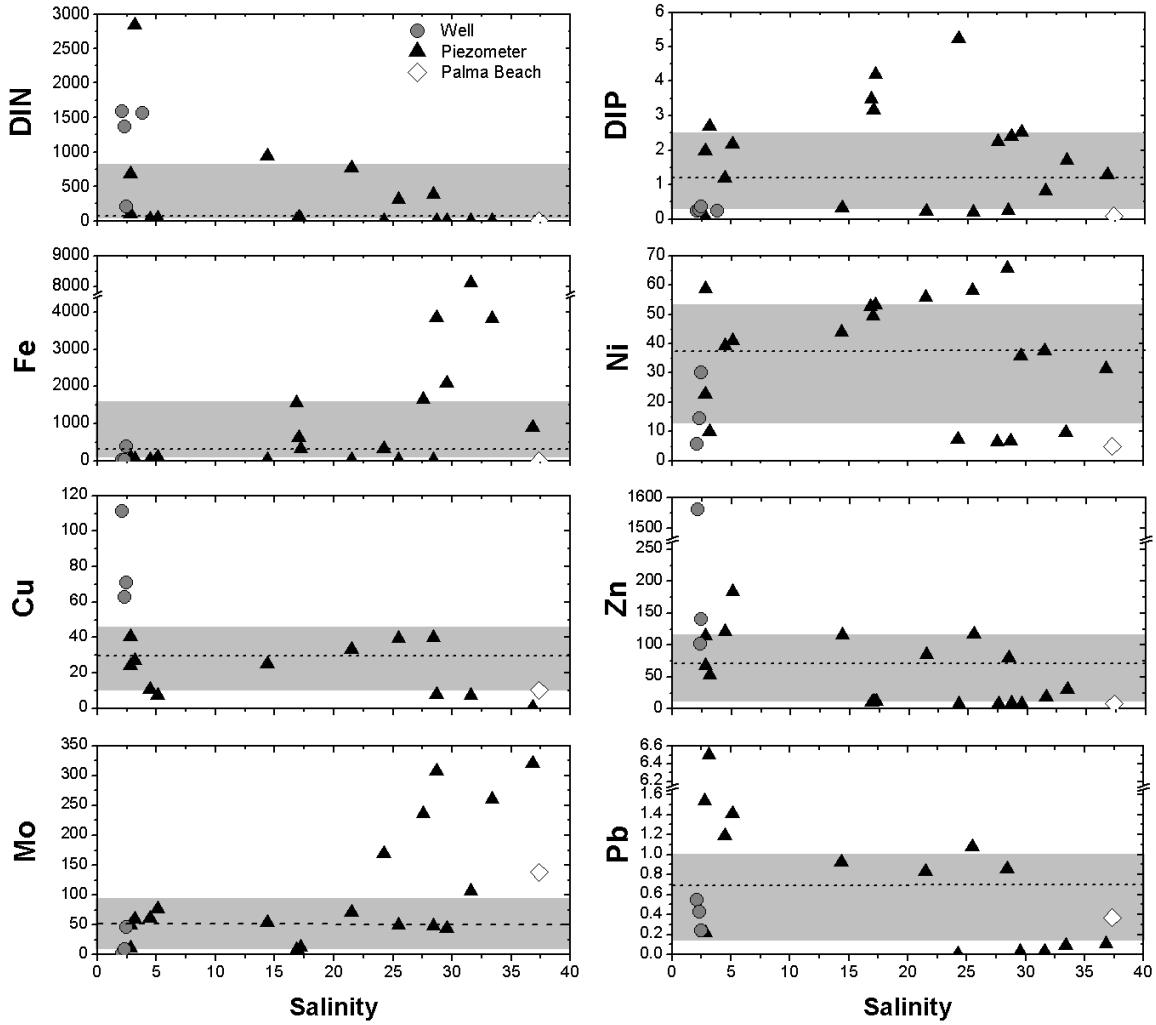

790

791

792 **FIGURE 7**

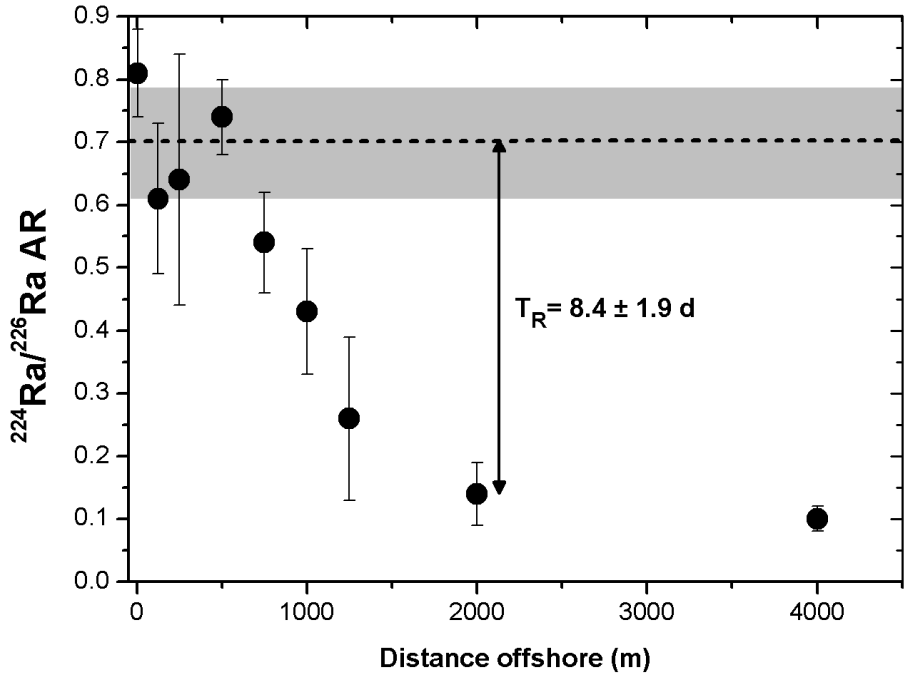

793

794

795 **FIGURE 8**

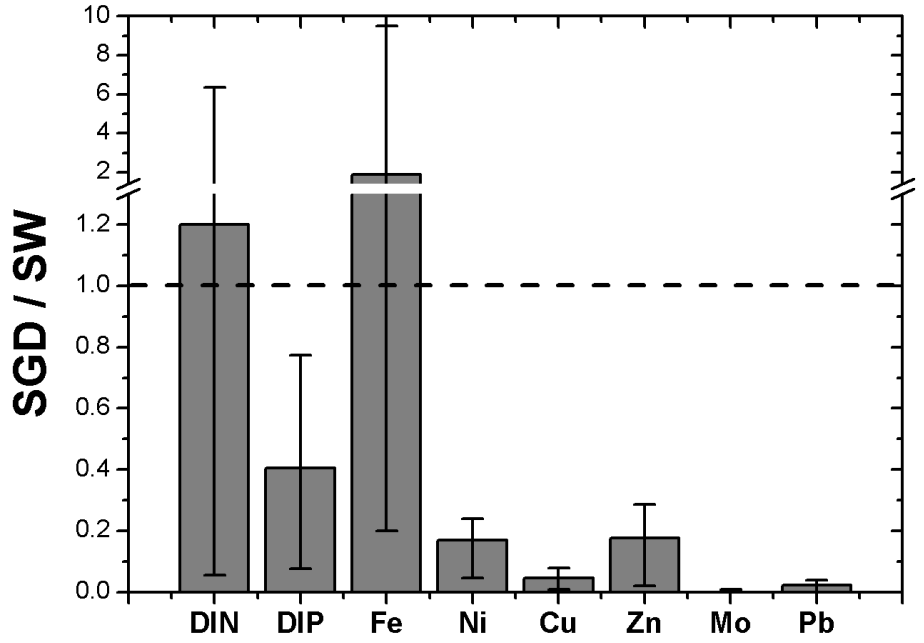

796

797

798

799 **FIGURE 9**

800

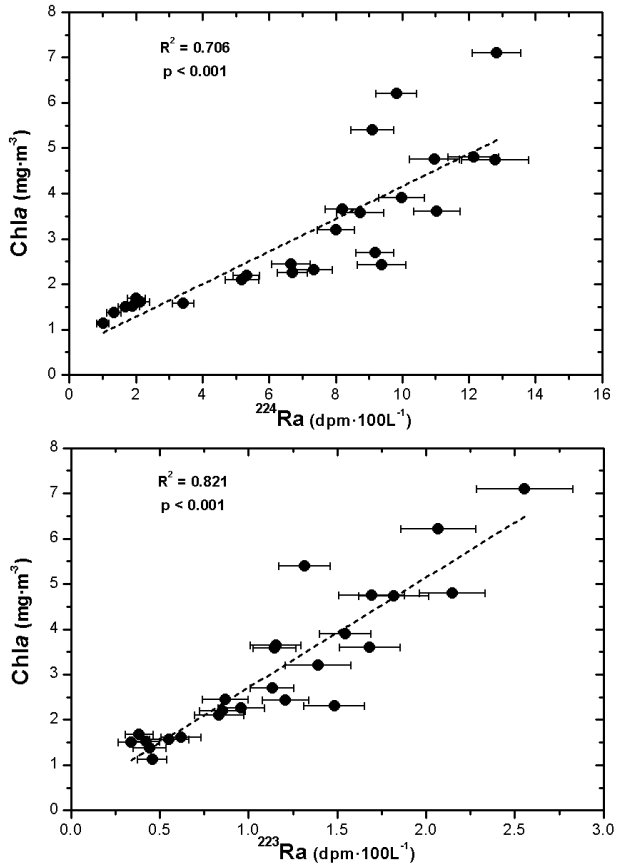

801